Retrieval of the molecular alignment distribution from THz generation

Ya-Ning Li,[1] Jin-Xu Du,[1] Lei Zhang [©],[2] Zhi-Hong Jiao,[1] Song-Feng Zhao [©],[1] and Guo-Li Wang [©][1,*]

[1]*College of Physics and Electronic Engineering, Northwest Normal University, Lanzhou 730070, China*
[2]*School of Mathematics and Physics, Lanzhou Jiaotong University, Lanzhou 730070, China*

Accurate characterization of molecular alignment distribution is critical for correctly understanding results in strong-field experiments involving molecules. In this study, we theoretically propose a method to retrieve the alignment distribution of transiently aligned molecules from their terahertz spectra using a genetic algorithm based on the photocurrent model. The feasibility of our retrieval approach relies on the observation, verified by both experiments and simulations, that molecular terahertz radiation yields are strongly modulated by the alignment degree, and accordingly, alignment distribution of molecules. We demonstrate that the precise determination of alignment distribution of molecules can be achieved across a wide range of terahertz frequencies and driving laser intensities, if terahertz radiation is measured at different pump-probe angles. Notably, our retrieval procedure is straightforward to implement as it only requires knowledge about ionization probabilities obtained from simulations.

I. INTRODUCTION

Molecular alignment is a crucial parameter in the field of physics and chemistry. Numerous research findings have demonstrated that molecular orientation and alignment play pivotal roles in the chemical reaction rate, reaction probability, and reaction products [1–3]. Various methods can be employed to achieve molecular alignment, including collision [4,5], electrostatic field [6,7], and laser driving [8–11]. Among these methods, laser driving has emerged as the most popular approach currently. In this scheme, the alignment does not occur immediately when the aligning laser pulse interacts with the molecule; instead, partial alignment occurs periodically in the form of fractional and full revivals after the aligning laser pulse has passed. Aligned molecules find applications not only in probing chemical reaction dynamics [12], but also extensively contribute to studying strong-field phenomena, such as high-order harmonic generation (HHG) [13,14], tomographic imaging [15,16], laser-induced electron diffraction [17,18], multiphoton and tunneling ionization [19], and so on. Accurate characterization of molecular alignment distribution (or the alignment degree) is essential for correctly interpreting these results.

Several methods have been proposed for estimating molecular alignment distribution [18,19]. Recently, it was suggested that the high harmonics generated during molecular transient alignment can be utilized to obtain the alignment distribution of molecules [20–24]. In Ref. [21], He *et al.* demonstrated that the calculations enable obtaining molecular orientation distribution by extracting the gas rotation temperature and the intensity of the pump laser from HHG experiments using sensitive dependence on the local minimum and maximum

generation time in the time-resolved high harmonic spectrum. Jin *et al.* [22] showed that the minimum values in the HHG spectrum of aligned CO_2 molecules are highly responsive to the degree of alignment enabling retrieval thereof. Guo *et al.* [23] also proposed utilizing the polarization properties of the harmonics emitted from aligned N_2 molecules to retrieve the alignment distribution. However, practical measurement limitations such as a small perpendicular component and efficiency of polarization measurement may restrict the accuracy of this method. Recently, Jiang *et al.* [24] introduced an alternative approach for obtaining alignment distribution from the harmonic spectra of aligned CO_2 molecules, which requires prior knowledge of the angular differential photoionization cross section of the molecule and pump-probe angle-dependent ionization probability.

In conjunction with HHG, terahertz (THz) waves can be simultaneously emitted when short laser pulses interact with the gas due to the time-varying current generated by the ionized free electrons under the influence of the driving laser field [25–27]. In this study, we present a potential method for retrieving the transiently aligned molecule's alignment distribution from THz radiation spectra. Unlike HHG that involves electron-parent ion recombination, THz radiation solely relies on an ionization process, making our proposed method relatively simpler and more user-friendly.

II. THEORETICAL METHODS

A. Alignment distribution of molecules by a pump laser

The alignment distribution of molecules excited by a relatively weak infrared laser (called a pump laser) can be precisely calculated by solving the time-dependent Schrödinger equation (TDSE) [28,29] by treating each molecule as a rigid rotor. For each initial rotational state of linear molecule, the

---

*wanggl@nwnu.edu.cn

TDSE is

$$i\frac{\partial \Psi_{JM}(\theta, \varphi, t)}{\partial t} = \left[B\mathbf{J}^2 - \frac{E_{\text{pump}}(t)^2}{2}(\alpha_\parallel \cos^2 \theta + \alpha_\perp \sin^2 \theta) \right] \Psi_{JM}(\theta, \varphi, t), \quad (1)$$

where $E_{\text{pump}}(t)$ is the electric field of the pump laser, J is the angular momentum operator, B is the rotational constant, $\alpha_\parallel$ and $\alpha_\perp$ are the anisotropic polarizabilities in parallel and perpendicular directions with respect to the molecular axis, respectively. θ and φ are the polar and azimuthal angles of the molecular axis in the frame attached to the pump laser field. Equation (1) is solved independently for each initial rotational state $|JM\rangle$ using the split operator method. After the pump laser is over, the rotational wave packet continues to propagate in the free space, and at the intervals of "rotational revivals" the molecules are nicely aligned or antialigned.

The time-dependent alignment distribution at a given gas temperature can be obtained as

$$\rho(\theta, t) = \sum_{JM} \omega_{JM} |\Psi_{JM}(\theta, \varphi, t)|^2, \quad (2)$$

where ω_{JM} is the weight according to the Boltzmann distribution in which the nuclear statistics and symmetry of the total electronic wave function are properly considered. The alignment distribution does not depend on the azimuthal angle φ for linear molecules.

The degree of alignment at a given time is defined in the pump-laser frame as

$$\langle \cos^2 \theta \rangle = \int_0^\pi \cos^2 \theta \rho(\theta) \sin \theta d\theta. \quad (3)$$

B. Molecular THz generation–plasma photocurrent model

When a strong probe laser pulse interacts with a gas, the electrons in the molecules are ionized to form a gas plasma, and the generated free electrons are accelerated by the laser field to form a transverse current $J(t)$, which oscillates with time and radiates electromagnetic waves, including waves in the THz frequency band. $J(t)$ can be computed as [30–32]

$$J(t) = \frac{e^2}{m_e} \int_{-\infty}^t \rho(t') E_{\text{prop}}(t') dt', \quad (4)$$

or equivalently [25–27]

$$J(t) = -\int_{-\infty}^t e v_e(t, t') d\rho(t'), \quad (5)$$

where $v_e(t, t')$ is the velocity of electron born at t' under the electric field $E_{\text{prop}}(t)$,

$$v_e(t, t') = -\frac{e}{m_e} \int_{t'}^t E_{\text{prop}}(t'') dt'', \quad (6)$$

with the assumption of the initial velocity of the ionized electron to be zero. Here, e and m_e are the elementary charge and electron mass, respectively. In Eq. (5), the increment of the electron density $\rho(t)$ during the interval between t and $t + dt$ is given by

$$\frac{d\rho(t)}{dt} = \omega(t)[\rho_0 - \rho(t)], \quad (7)$$

where ρ_0 is the initial density of the molecules. If the pump and probe laser polarizations are parallel, the alignment-dependent ionization rate $\omega(t)$ can be calculated by coherently adding the weighted contribution from different alignments by [33]

$$\omega(t) = C \int \omega[\theta, E_{\text{prop}}(t)] \rho(\theta, t) \sin \theta d\theta, \quad (8)$$

where C is a constant and θ is the angle between the laser polarization and the molecular axis for linear molecules. The pure angle-dependent ionization rate $\omega[\theta, E_{\text{prop}}(t)]$ is obtained with the molecular Ammosov-Delone-Krainov (MO-ADK) model [34,35]. If the polarizations of the pump and probe lasers are not the same, but with an angle of α, the alignment distribution $\rho(\theta, t)$ can be expressed in the probe-laser frame [36,37]. The relationship between θ and (θ', φ') has the form

$$\cos \theta = \cos \theta' \cos \alpha + \sin \theta' \sin \alpha \cos \varphi'. \quad (9)$$

The alignment distribution is then transformed into a frame attached to the probe laser as

$$\rho(\alpha, \theta', \varphi') = \rho[\theta(\alpha, \theta', \varphi')]. \quad (10)$$

After averaging the ionization rate over the molecular angular distribution, the averaged ionization rate can be obtained as

$$\bar{\omega}(\alpha, t) = \int_0^\pi \int_0^{2\pi} \omega[\theta', E_{\text{prop}}(t)] \rho(\alpha, \theta', \varphi') \sin \theta' d\theta' d\varphi'. \quad (11)$$

At a given alignment angle α, the THz spectrum can be calculated by

$$P_{\text{THz}}(\omega) = \left| \widehat{F} \left[\frac{d\langle J(t) \rangle}{dt} \right] \right|^2, \quad (12)$$

where $\widehat{F}$ represents the Fourier transform. Because the above model excludes macroscopic effects, it is appropriate for simulating THz generation from thin low-density plasma [38].

C. Retrieve procedure of alignment distribution

To retrieve the alignment distribution function $\rho(\theta)$ of homonuclear diatomic molecules from measured THz radiation, we expand $\rho(\theta)$ at a given time as a polynomial of $\cos^2 \theta$

$$\rho(\theta) = a_0 + \sum_1^{n_{\max}} a_n \cos^{2n} \theta, \quad (13)$$

where $a_n (n = 0, \ldots, n_{\max})$ is the expansion coefficient. Thus to retrieve the alignment distribution is actually to determine these coefficients.

We choose a genetic algorithm (GA) to find the parameters of $\{a_n\}$ in Eq. (13). GA, a well-known evolutionary algorithm capable of dealing with highly nonlinear response functions, has been widely used to study strong-field phenomena [39–47]. It begins with a population of randomly generated individuals; better individuals are selected from the current generation by evaluating each individual's fitness function and are then employed in the next generation. Once an acceptable fitness level is reached, the evolution process is
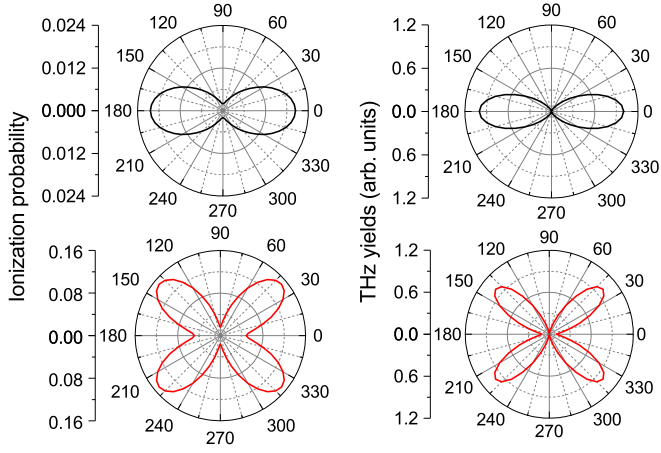
FIG. 1. Ionization probability (left column) and normalized THz yields (right column) as a function of the angle between the probe laser field direction and the molecular axis for the N_2 molecule (top row) and O_2 molecule (bottom row).

terminated. In our retrieval method, we use the THz yields at a fixed frequency range versus the pump-probe angle to construct the fitness function, which is defined as

$$F\{a_n\} = 1 / \sum_i |P_{\text{THz\_input}}(\alpha_i) - P_{\text{retrieval}}(\alpha_i)|^2, \qquad (14)$$

where i is the index of the pump-probe angle α, $P_{\text{THz\_input}}$ is the input data for experimental THz intensity, and $P_{\text{retrieval}}(\alpha_i)$ is the calculated ones by using parameters of $\{a_0, a_1, \ldots, a_{n_{\max}}\}$.

III. RESULTS AND DISCUSSION

A. Single molecules THz generation: THz yield dependence on the ionization probability and probe angle

Unlike atoms, molecules in general are not isotropic systems, and the ionization probability can be strongly influenced by the angle between the molecular axis and the driving laser electric field vector. Therefore, the generated THz yield strongly depends on this angle as well. For N_2, the valence electron is a σ_g orbital, and its electron cloud is preferentially aligned along the internuclear axis. Thus, when the molecular axis is along the laser polarization direction, the electronic density is at its maximum and the electron is most easily ionized. The situation is different for O_2. Its valence electron is a π_g orbital. When the molecular axis coincides with the laser polarization direction, there is little valence electron density. However, when the field direction is at $40°$ with respect to the molecular axis, the electron cloud will have maximum density, resulting in the highest ionization probability.

Figure 1 illustrates the dependence of the THz yield $[\int_0^{10\text{THz}} P_{\text{THz}}(\omega) d\omega$, with only the highest occupied molecular orbital (HOMO) included in the simulation] of N_2 and O_2 molecules on the ionization probability and angles between the polarization direction of probe laser field and the molecular axis. In the simulation of THz generation, we utilize a 25-fs two-color laser pulse, similar to the one used in the experiment of Kim *et al.* [33]. The wavelengths used are 800 nm and 400 nm, respectively. The total laser peak intensity is
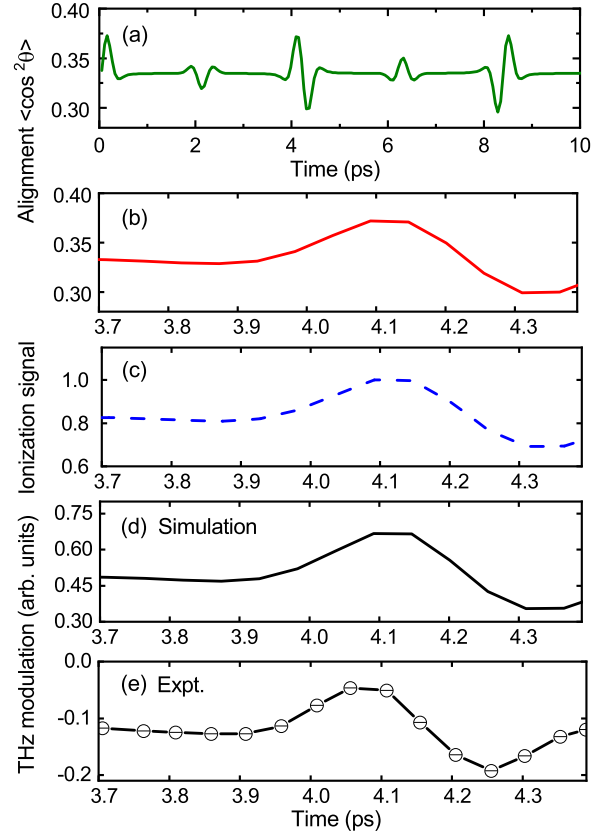

FIG. 2. (a) Calculated alignment degree of N_2 molecule at times during and after pump laser. (b) The alignment degree during the time delay of 3.7 ps to 4.4 ps. (c) Alignment-dependent N_2 ionization signal. (d) The simulated THz signal around the half revival period of N_2. (e) The measured THz modulation from Ref. [33].

1.1×10^{14} W/cm^2 with a ratio of $I_2/I_1 = 0.1$. The phase difference between the two components is 0.5π. It is evident that there is a positive correlation between the strength of THz radiation and the ionization probability of molecules. In other words, higher ionization corresponds to stronger THz radiation and vice versa. Additionally, THz strength is heavily influenced by the angle between the polarization direction of the probe laser and the molecular axis. These correlations persist after accounting for molecular orientation and are consistent with experimental findings [48], forming the theoretical basis of our proposal to retrieve the molecular alignment distribution from their generated THz waves.

B. THz generation from aligned molecules: Simulation versus experiment

In the molecular THz generation experiment, the molecules are first aligned by a weak pump laser pulse before being exposed to a strong probe laser field. In Figs. 2(a) and 2(b), we show the calculated N_2 alignment degree $\langle \cos^2 \theta \rangle$ as a function of time during and after the pump pulse, which is a 25-fs two-color field with a total intensity of 0.3×10^{14} W/cm^2 and a ratio of $I_2/I_1 = 0.1$. The simulation uses a gas temperature of 150 K. Under these conditions, the curve exhibits a full revival near about 8.5 ps, as well as a half revival near 4.1 ps.
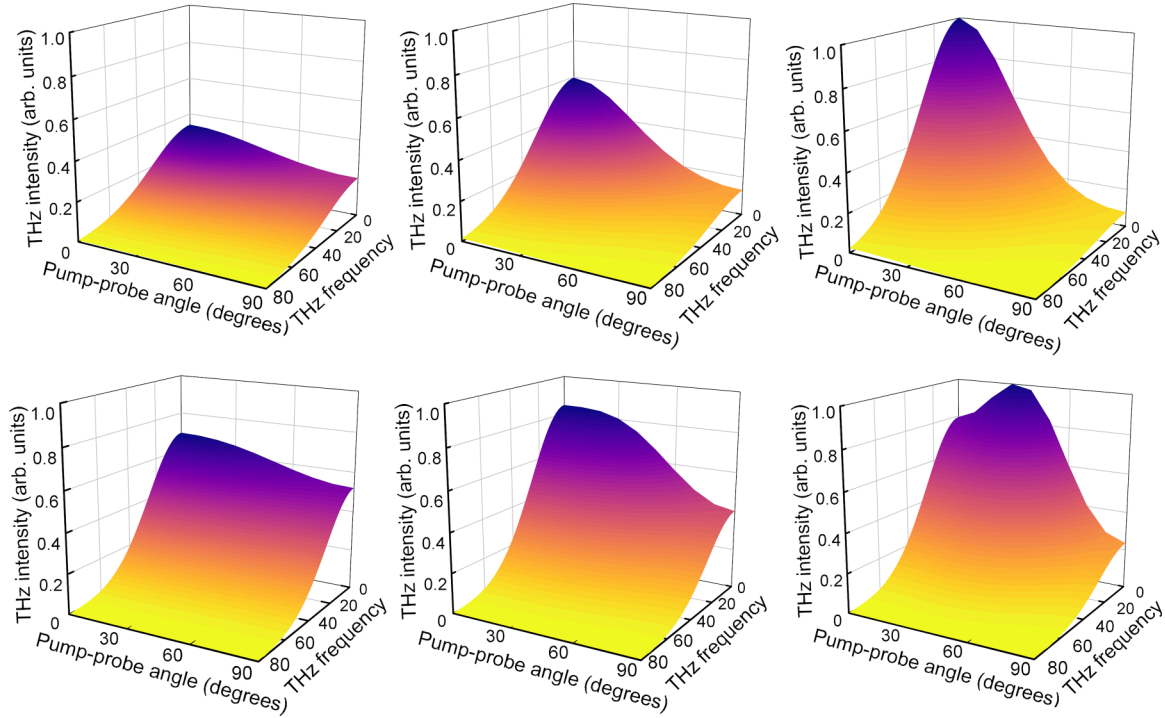
FIG. 3. THz spectra from aligned N_2 molecules (top row) and O_2 molecules (bottom row) as a function of pump-probe angles. The alignment degree is $\langle \cos^2 \theta \rangle \approx 0.40$ (left column), 0.55 (middle column) and 0.70 (right column).

Near these revivals, the maximal alignment degree reaches $\langle \cos^2 \theta \rangle \approx 0.37$. The flat parts represent the isotropic distribution with $\langle \cos^2 \theta \rangle \approx 1/3$. Figure 2(c) depicts the ionization degree varying with the delay time near half revival, which is also induced by a two-color probe field similar to that used in the Fig. 1, but with a parallel polarization to the pump laser. It behaves similarly to the degree of alignment, i.e., the more N_2 molecules aligned to the probe laser polarization direction, the more free electrons are generated. This is in accordance with the single molecule results shown in Fig. 1. Figure 2(d) shows the calculated THz signal, which exhibits a very similar behavior to the ionization signal. The dependence of THz modulations on ionization signals and molecular alignment distribution is completely consistent with the experimental findings [33]. In Fig. 2(e), we present the experimental demonstration of THz modulation with time delays. Some discrepancy in the peak position between the simulation and experiment could be due to the discordance of parameters (total laser intensity, gas temperature) adopted in the two investigations. Furthermore, in Ref. [33], the time delay in the molecular THz generation differs from that in the molecule alignment.

C. "Experimental" THz data for the retrieval of molecular alignment distribution

To retrieve molecular alignment distribution, we request some THz data at a certain alignment degree and multiple pump-probe angles. We consider simulated THz spectra as "experimental" ones based on the consistency between experiment and simulation. Figure 3 depicts the simulated N_2 and O_2 THz spectra as a function of the frequency (0 to 100 THz) and pump-probe angles ($0°$–$90°$, with a step of $5°$), for three alignment degrees of $\langle \cos^2 \theta \rangle \approx 0.40$, 0.55, and 0.70, respectively. Such values are taken from the alignment degree at full revival from a specific alignment experiment, which is possible with appropriate pump laser and gas temperature (see Table I). THz yields are normalized with respect to the highest THz intensity over the entire frequency bands. The probe lasers are the same as those used in Fig. 2. For N_2 molecules, the THz radiation decreases as the probe angle increases, for both alignment degrees. At the same time, the higher the alignment degree, the stronger the THz radiation. For the O_2 molecule, the ionization is the strongest when the angle between the probe laser and the molecular axis is $40°$. Therefore, the THz radiation strength depends on both the alignment degree and probe angle. When $\langle \cos^2 \theta \rangle = 0.40$, 0.55, the THz radiation at $0°$ is stronger than that at other angels. But for $\langle \cos^2 \theta \rangle = 0.70$, the strongest THz radiation is at $\sim 35°$.

TABLE I. Parameters used to align the N_2 and O_2 for the THz generation. The aligning pulse is an 800 nm + 400 nm dual-color laser field, intensity ratio and phase delay between two components is fixed as $I_2/I_1 = 0.1$ and 0.0π, respectively.

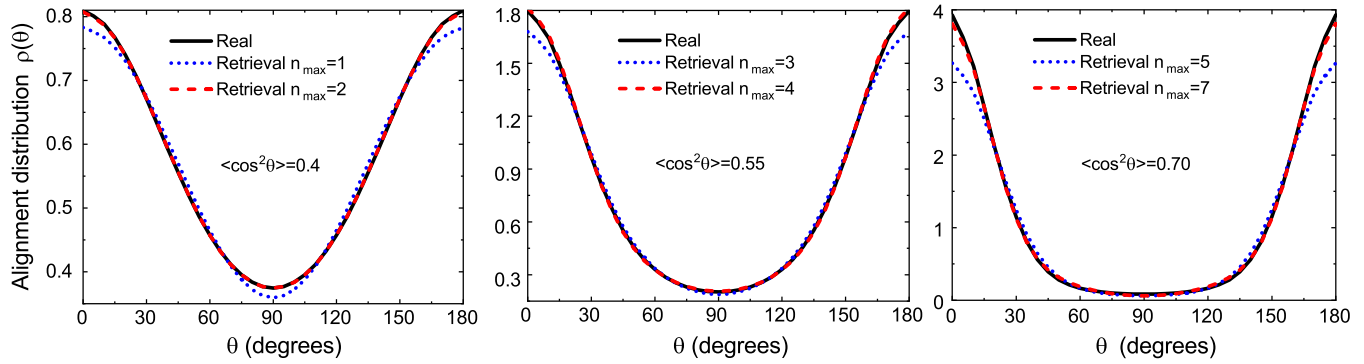|	Total intensity	Pulse width	Temperature	$\langle \cos^2 \theta \rangle$
N_2	0.3×10^{14} W/cm^2	15 fs	100 K	0.40
	0.5×10^{14} W/cm^2	26 fs	50 K	0.57
	0.7×10^{14} W/cm^2	28 fs	30 K	0.70
O_2	0.5×10^{14} W/cm^2	14 fs	180 K	0.41
	0.6×10^{14} W/cm^2	24 fs	100 K	0.56
	0.8×10^{14} W/cm^2	28 fs	50 K	0.71

FIG. 4. Retrieved molecular alignment distribution function $\rho(\theta)$ of aligned N_2 molecules by using the THz radiation at 10 THz. The different n_{max} is required for the different alignment degree $\langle \cos^2 \theta \rangle$ to achieve a convergent result in the retrieval.

D. Retrieval of alignment distributions of N_2 and O_2

1. Retrieval at a given THz frequency: Validity test

To begin, we use THz radiation at 10 THz of N_2 shown in Fig. 3 as the "input" data to test the validity of our retrieval approach. Figure 4 depicts the retrieved alignment distributions. The "input" (or "real") alignment distributions are also presented for comparison. Obviously, if the n_{max} in Eq. (13) is large enough for each given degree of the alignment (we set $0 \leqslant a_n \leqslant 1$ in current optimizations), the angular distribution can be reliably recovered (relative error less than 4% at $0°$). The higher the degree of alignment, the bigger the n_{max} required. For $\langle \cos^2 \theta \rangle = 0.70$, for example, at least seven expansion coefficients are needed.

2. Retrieval with THz radiation from wide frequency range

The ease of retrieval in a practical application is affected by whether the alignment distribution can be extracted over a wide range of THz waves. In Fig. 5, we show the alignment distributions for N_2 and O_2 retrieved from THz radiations at 5 THz and 10 THz, and THz yield between 0 to 10 THz. The retrieved distributions all agree quite well with the "real" ones for varied $\langle \cos^2 \theta \rangle$ and THz energies employed. This means that there is no specific requirement in our retrieval procedure for the THz range. In the case of N_2 and O_2, the maximum expanded items in Eq. (13) are $n_{max} = 2, 4, 7$ for $\langle \cos^2 \theta \rangle = 0.40, 0.55, 0.70$, and $n_{max} = 3, 4, 8$ for $\langle \cos^2 \theta \rangle = 0.41, 0.56, 0.71$, respectively. It is worth noting that the harmonics at the Cooper minimum are often required in the alignment retrieval from HHG [24].
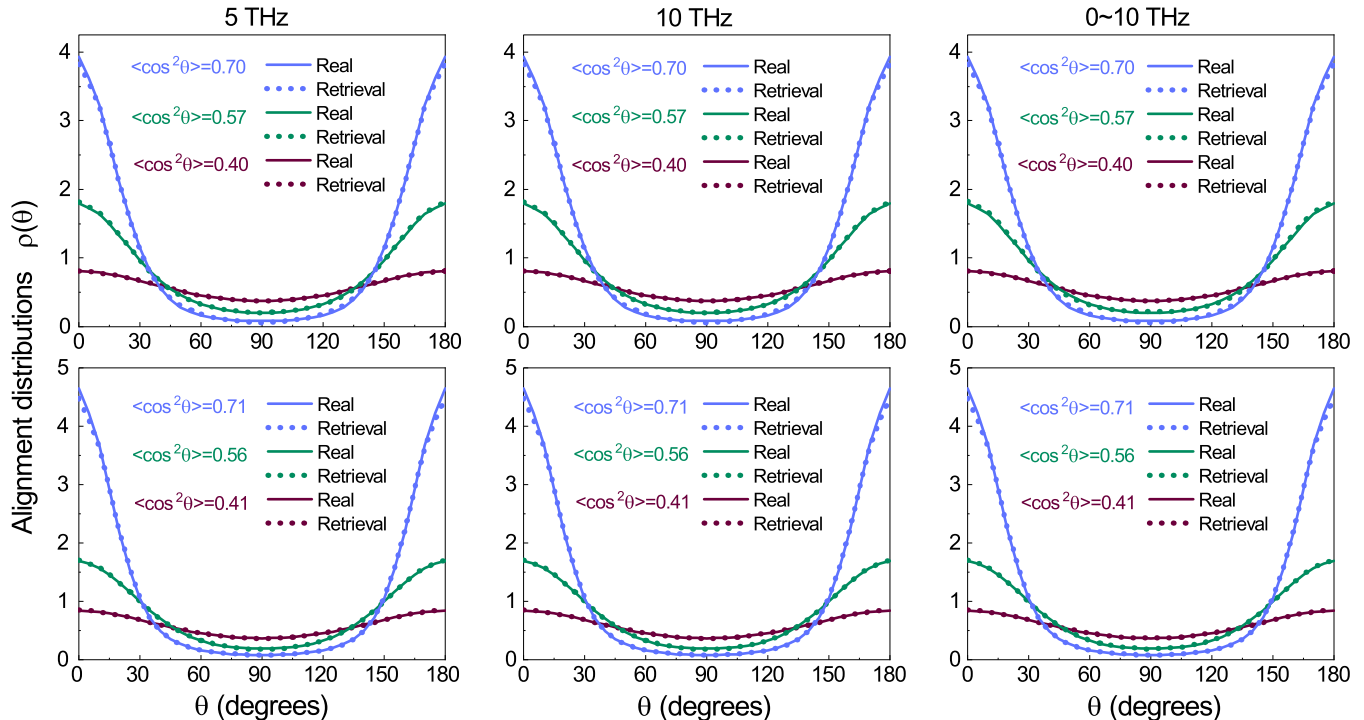

FIG. 5. Comparison of the real and the retrieved alignment distributions for N_2 (top row) and O_2 (bottom row). The THz radiations at different frequency are used, left column: 5 THz; middle column: 10 THz; right column: 0 to 10 THz.
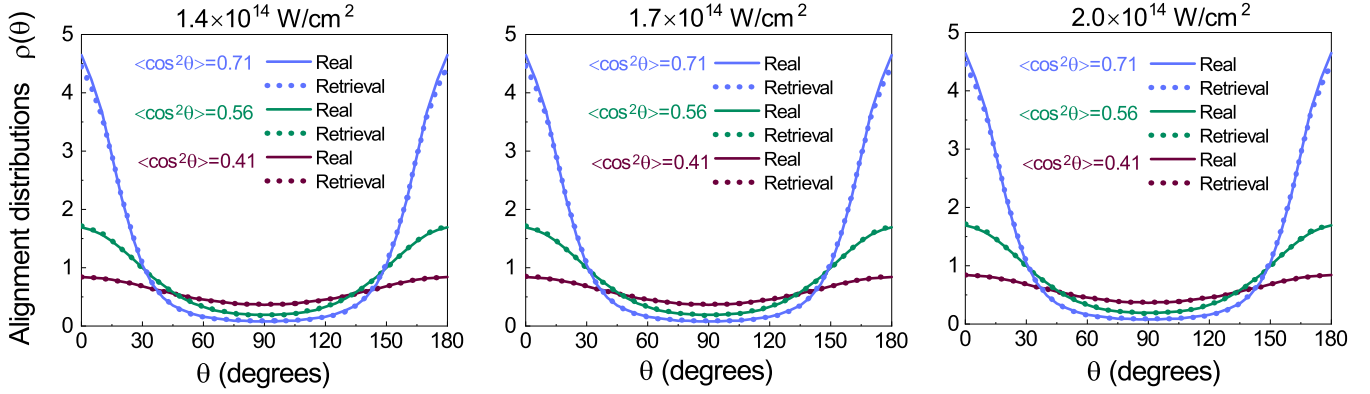
FIG. 6. Comparison of real and retrieved alignment distributions at higher probe laser intensities. The [0 to 10 THz] THz yields from O_2 are taken as "experimental" ones. The total intensity of the probe laser in the retrieval is $1.4 \times 10^{14}\,\text{W/cm}^2$, $1.7 \times 10^{14}\,\text{W/cm}^2$, $2.0 \times 10^{14}\,\text{W/cm}^2$.

3. Retrieve $\rho(\theta)$ at higher probe laser intensity

To generate stronger THz radiation, a probe laser with higher intensity may be required. Given this, we simulate THz spectra of aligned O_2 with total laser intensity of $1.4 \times 10^{14}\,\text{W/cm}^2$, $1.7 \times 10^{14}\,\text{W/cm}^2$, and $2.0 \times 10^{14}\,\text{W/cm}^2$, while keeping the other laser parameters and gas temperature the same as those in Fig. 3. The final retrieved results are shown in Fig. 6. For $\langle \cos^2 \theta \rangle = 0.71$, $n_{\max}$ is now increased to 9. When the laser intensity increases to the higher one, the retrieved distributions still agree very well with the "real" ones. The worst case is a relative error of less than 4.3% at $0°$ and $180°$ degrees, when the alignment degree $\langle \cos^2 \theta \rangle = 0.71$.

4. Retrieve $\rho(\theta)$ with uncertain probe laser intensity

Our retrieval method relies on an accurate alignment-dependent ionization probability estimated with a given probe laser intensity. However, determining laser intensity accurately and directly in an experiment for a focused ultrafast laser pulse is extremely challenging. A 10% accuracy in the determination is normal. Is it still possible for our methods to be valid if the laser intensity has such a large uncertainty? Let us respond to this question. We employ the [0 THz, 10 THz] yields from O_2 generated by a probe laser with an intensity of $1.4 \times 10^{14}\,\text{W/cm}^2$ as our "experimental" data, but with a 8% uncertainty for the laser intensity, namely, $1.3 \times 10^{14}\,\text{W/cm}^2$ and $1.5 \times 10^{14}\,\text{W/cm}^2$ are used in the retrieval. The retrieved results are shown in Figs. 7(a) to 7(c). As shown in the figure, the laser intensity does significantly affect the outcomes of the extraction. When the retrieving laser intensity is higher than the real one, the ionization is enhanced, the retrieved alignment distribution is reduced, and vice versa. The relative error between retrieved and real $\rho(\theta)$ is in the range of $[-32\%, 46\%]$ for $\langle \cos^2 \theta \rangle = 0.41$ and $[-30\%, 46\%]$ for $\langle \cos^2 \theta \rangle = 0.56$, and $[-35\%, 59\%]$ for $\langle \cos^2 \theta \rangle = 0.71$. To clarify, the greatest error does not occur at $\theta = 0°$. At $\theta = 90°$, the maximal relative error for total ionization probability at the end of laser pulse is 34% and 28%, respectively [Fig. 7(d)]. If we take the mean value of the alignment distributions extracted with two inaccurate laser intensities, it then very closely matches the real value. This indicates that, even if we

use a laser intensity with greater uncertainty in the extraction process, the average (or fitting) result will still be close to the true value.
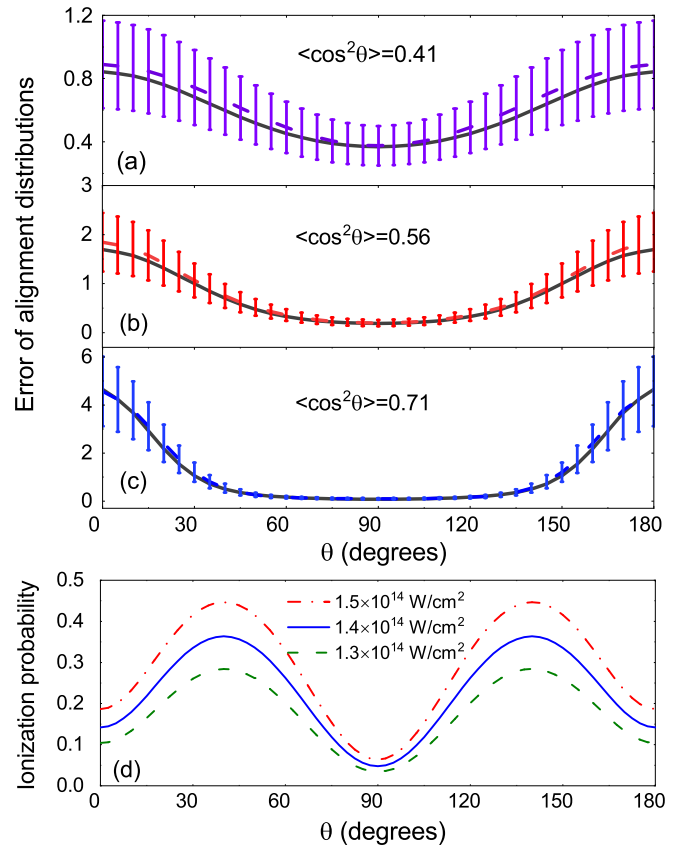

FIG. 7. [(a)–(c)] Alignment distribution $\rho(\theta)$ of O_2. For each alignment degree, the black solid line is the real one or retrieved from THz generation with accurate probe laser intensity of $1.4 \times 10^{14}\,\text{W/cm}^2$, the error bar represents the $\rho(\theta)$ retrieved by using trial intensity of $1.3 \times 10^{14}\,\text{W/cm}^2$ and $1.5 \times 10^{14}\,\text{W/cm}^2$ in the retrieval, the dashed line is the mean value of the error bar. (d) The ionization probability at the end of the probe pulse calculated by using the MO-ADK theory for three laser intensities.
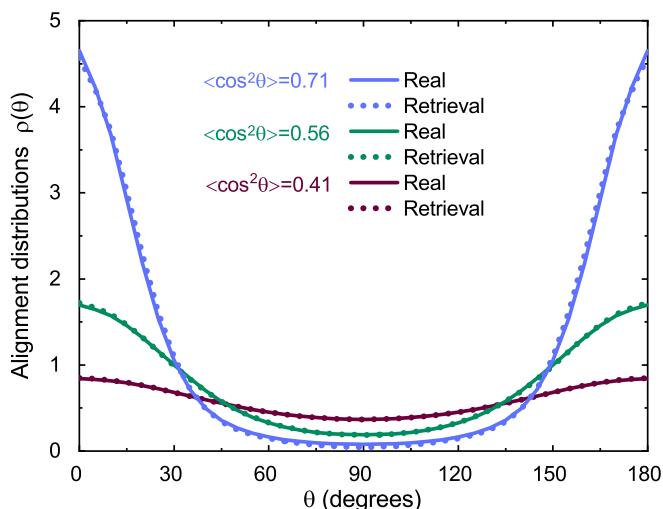
FIG. 8. (a) Retrieved alignment distribution of O_2 molecules with 10-THz radiations at four α angles: $0°$, $30°$, $60°$, $90°$ for $\langle \cos^2 \theta \rangle = 0.41$, 0.56, and $0°$, $10°$, $20°$, $30°$ for $\langle \cos^2 \theta \rangle = 0.71$. The intensity for the probe laser is 1.4×10^{14} W/cm^2.

5. Retrieve $\rho(\theta)$ with fewer α angles

With 19 pump-probe angles, we establish good agreement between the retrieved and real molecule alignment distributions in the preceding demonstration. Is it possible to obtain such consistency with fewer angles between two lasers? From Fig. 3 one can see that THz signals monotonically decrease as α increases from $0°$ to $90°$ at a given THz frequency in the cases of N_2, and lower alignment degrees for O_2 [Figs. 3(a)

to 3(e)]. In these cases, precise alignment distributions can be extracted completely by employing THz radiations at four α angles ranging from $0°$ to $90°$. For $\langle \cos^2 \theta \rangle = 0.71$ for O_2, THz radiation does not vary monotonically with α over the entire angle range. In this case, if we choose a reasonable α range, such as $0°-30°$, the molecular alignment distribution can still be accurately retrieved with only four α angles. Consider THz radiation at 10 THz, as illustrated in Fig. 8.

IV. CONCLUSION

In conclusion, we proposed theoretically a THz application for retrieving molecular alignments via THz generation. We revisited the two-color N_2 THz experimental results in Ref. [33] to demonstrate the reliability of the simulation model we employed. We achieved very good consistency between the simulation and experiment, which both showed that THz radiation is extremely sensitive to the probe-pump laser delay time and, consequently, molecular alignment degree. Thus, we show that throughout a broad range of THz radiation frequency and probe laser intensity, the alignment distribution of transiently aligned molecules at a given time can be precisely retrieved from the probe-pump-angle-dependent THz spectra. Due to the fact that we simply need to know the probability of the molecules being ionized, our retrieval procedure is rather simple. It enriches the measuring means of molecular orientation distribution.

[1] P. R. Brooks, Science **193**, 11 (1976).

[2] R. D. Levine, R. B. Bernstein, and Y. T. Lee, Phys. Today **41**, 90 (1988).

[3] R. B. Bernstein, *Chemical Dynamics via Molecular Beam and Laser Techniques* (Oxford University Press, New York, 1982).

[4] D. P. Pullman, B. Friedrich, and D. R. Herschbach, J. Chem. Phys. **93**, 3224 (1990).

[5] V. Aquilanti, D. Ascenzi, M. de Castro Vitores, F. Pirani, and D. Cappelletti, J. Chem. Phys. **111**, 2620 (1999).

[6] K. Kramer and R. Bernstein, J. Chem. Phys. **42**, 767 (1965).

[7] B. Friedrich and D. Herschbach, Z. Phys. D: At., Mol. Clusters **18**, 153 (1991).

[8] D. Normand, L. Lompre, and C. Cornaggia, J. Phys. B: At. Mol. Opt. Phys. **25**, L497 (1992).

[9] S. Banerjee, G. R. Kumar, and D. Mathur, Phys. Rev. A **60**, R3369(R) (1999).

[10] B. Friedrich and D. Herschbach, J. Chem. Phys. **111**, 6157 (1999).

[11] B. Friedrich and Herschbach, J. Phys. Chem. A **103**, 10280 (1999).

[12] H. Ihee, V. A. Lobastov, U. M. Gomez, B. M. Goodson, R. Srinivasan, C. Ruan, and A. H. Zewail, Science **291**, 458 (2001).

[13] Y. Mairesse, J. Higuet, N. Dudovich, D. Shafir, B. Fabre, E. Mével, E. Constant, S. Patchkovskii, Z. Walters, M. Y. Ivanov, and O. Smirnova, Phys. Rev. Lett. **104**, 213601 (2010).

[14] B. K. McFarland, J. P. Farrell, P. H. Bucksbaum, and M. Guhr, Science **322**, 1232 (2008).

[15] J. Itatani, J. Levesque, D. Zeidler, H. Niikura, H. Pćpin, J. Kieffer, P. B. Corkum, and D. M. Villeneuve, Nature (London) **432**, 867 (2004).

[16] C. Vozzi, M. Negro, F. Calegari, G. Sansone, M. Nisoli, S. De Silvestri, and S. Stagira, Nat. Phys. **7**, 822 (2011).

[17] C. I. Blaga, J. Xu, A. D. DiChiara, E. Sistrunk, K. Zhang, P. Agostini, T. A. Miller, L. F. DiMauro, and C. D. Lin, Nature (London) **483**, 194 (2012).

[18] M. G. Pullen, B. Wolter, A.-T. Le, M. Baudisch, M. Hemmer, A. Senftleben, C. D. Schröter, J. Ullrich, R. Moshammer, C. D. Lin *et al.*, Nat. Commun. **6**, 7262 (2015).

[19] D. Pavičić, K. F. Lee, D. M. Rayner, P. B. Corkum, and D. M. Villeneuve, Phys. Rev. Lett. **98**, 243001 (2007).

[20] Y. He, L. He, P. Lan, B. Wang, L. Li, X. Zhu, W. Cao, and P. Lu, Phys. Rev. A **99**, 053419 (2019).

[21] Y. He, L. He, P. Wang, B. Wang, S. Sun, R. Liu, B. Wang, P. Lan, and P. Lu, Opt. Express **28**, 21182 (2020).

[22] C. Jin, S.-J. Wang, X. Zhao, S.-F. Zhao, and C. D. Lin, Phys. Rev. A **101**, 013429 (2020).

[23] X. Guo, C. Jin, Z. He, J. Yao, X.-X. Zhou, and Y. Cheng, Opt. Express **29**, 1613 (2021).

[24] C. Jiang, H. Jiang, Y. Chen, B. Li, C. D. Lin, and C. Jin, Phys. Rev. A **105**, 023111 (2022).

[25] K. Kim, J. H. Glownia, A. J. Taylor, and G. Rodriguez, Opt. Express **15**, 4577 (2007).

[26] K. Kim, A. Taylor, J. Glownia, and G. Rodriguez, Nature Photon. **2**, 605 (2008).

[27] K. Kim, Phys. Plasmas **16**, 056706 (2009).

[28] H. Stapelfeldt and T. Seideman, Rev. Mod. Phys. **75**, 543 (2003).

[29] C. Jin, A.-T. Le, S.-F. Zhao, R. R. Lucchese, and C. D. Lin, Phys. Rev. A **81**, 033421 (2010).

[30] F. Brunel, J. Opt. Soc. Am. B **7**, 521 (1990).

[31] V. B. Gildenburg and N. V. Vvedenskii, Phys. Rev. Lett. **98**, 245002 (2007).

[32] H.-C. Wu, J. Meyer-ter-Vehn, and Z.-M. Sheng, New J. Phys. **10**, 043001 (2008).

[33] Y. S. You, T. I. Oh, A. B. Fallahkhair, and K. Y. Kim, Phys. Rev. A **87**, 035401 (2013).

[34] X. M. Tong, Z. X. Zhao, and C. D. Lin, Phys. Rev. A **66**, 033402 (2002).

[35] S.-F. Zhao, C. Jin, A.-T. Le, T. F. Jiang, and C. D. Lin, Phys. Rev. A **82**, 049903(E) (2010).

[36] A.-T. Le, R. R. Lucchese, S. Tonzani, T. Morishita, and C. D. Lin, Phys. Rev. A **80**, 013401 (2009).

[37] M. Lein, R. De Nalda, E. Heesel, N. Hay, E. Springate, R. Velotta, M. Castillejo, P. Knight, and J. Marangos, J. Mod. Opt. **52**, 465 (2005).

[38] C. Meng, W. Chen, X. Wang, Z. Lü, Y. Huang, J. Liu, D. Zhang, Z. Zhao, and J. Yuan, Appl. Phys. Lett. **109**, 131105 (2016).

[39] X. Chu and S.-I. Chu, Phys. Rev. A **64**, 021403(R) (2001).

[40] D. Yoshitomi, J. Nees, N. Miyamoto, T. Sekikawa, T. Kanai, G. Mourou, and S. Watanabe, Appl. Phys. B **78**, 275 (2004).

[41] A. B. Yedder, C. Le Bris, O. Atabek, S. Chelkowski, and A. D. Bandrauk, Phys. Rev. A **69**, 041802(R) (2004).

[42] O. Boyko, C. Valentin, B. Mercier, C. Coquelet, V. Pascal, E. Papalazarou, G. Rey, and P. Balcou, Phys. Rev. A **76**, 063811 (2007).

[43] S. Eyring, C. Kern, M. Zürch, and C. Spielmann, Opt. Express **20**, 5601 (2012).

[44] L. E. Chipperfield, J. S. Robinson, J. W. G. Tisch, and J. P. Marangos, Phys. Rev. Lett. **102**, 063003 (2009).

[45] E. Balogh, B. Bódi, V. Tosa, E. Goulielmakis, K. Varjú, and P. Dombi, Phys. Rev. A **90**, 023855 (2014).

[46] C. Jin and C. D. Lin, Chin. Phys. B **25**, 094213 (2016).

[47] J.-X. Du, G.-L. Wang, X.-Y. Li, Z.-H. Jiao, S.-F. Zhao, and X.-X. Zhou, Phys. Rev. A **108**, 023101 (2023).

[48] Y. Huang, C. Meng, X. Wang, Z. Lü, D. Zhang, W. Chen, J. Zhao, J. Yuan, and Z. Zhao, Phys. Rev. Lett. **115**, 123002 (2015).